Predicting an Ultraviolet-Terahertz Double Resonance Spectrum of Formaldehyde

by

Emily E. Fenn

Submitted to the Department of Chemistry
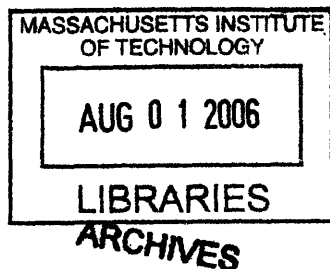in partial fulfillment of the requirements for the degree of

Bachelor of Science in Chemistry

at the

Massachusetts Institute of Technology

June 2006

© 2006 Massachusetts Institute of Technology

Author..
Department of Chemistry
12 May 2006

ɔ

Certified by...
Robert W. Field
Haslam and Dewey Professor of Chemistry
Thesis Supervisor

<

Accepted by...
Sylvia T. Ceyer
Chairman, Departmental Committee on Undergraduate Students

Predicting an Ultraviolet-Terahertz Double Resonance Spectrum of Formaldehyde

by

Emily E. Fenn

Submitted to the Department of Chemistry
on 12 May 2006
in Partial Fulfillment of the Requirements
for the Degree of
Bachelor of Science in Chemistry

ABSTRACT

In preparation for performing a triple resonance experiment to study the Rydberg states of calcium monofluoride (CaF), a double resonance spectrum of formaldehyde will be recorded. A dye laser will populate a level in formaldehyde's first electronically excited state, and pure rotational transitions will be induced by applying a terahertz electric field. A terahertz spectrometer has been built for this purpose, and the principles of terahertz spectroscopy are described.

The 4^1_0 vibronically allowed transition of the $\tilde{A}\,^1A_2 \leftarrow \tilde{X}\,^1A_1$ electronic transition was chosen for study. The dye laser will be tuned to 28307.13 cm^{-1} (353.2679 nm) within this band in order to transfer population from the J"= 9, K"= 0 level in the ground state to the J'= 9, K'=1 level in the excited state, according to b-type selection rules for electronic transitions. A Boltzmann distribution was used to determine that J" = 9, K"=0 was the most populated state, and 50% of the molecules from this level will be transferred to the excited state.

The new population differences created after electronic excitation will allow four rotational lines ($J_{9\leftarrow 8, K=0}$ and $J_{9\leftarrow 10, K=0}$ in the ground state, and $J_{10\leftarrow 9, K=1}$ and $J_{8\leftarrow 9, K=1}$ in the excited state) to experience a significant gain in absorption coefficient compared to all other rotational transitions occurring in the ground state. These new absorption coefficients are calculated and compared against those for the ground state spectrum without electronic excitation, showing about a factor of 10 increase. The changes in the THz electric field as it propagates through the sample of formaldehyde are also described.

Thesis Supervisor: Robert W. Field
Title: Haslam and Dewey Professor of Chemistry

For Corey Lowen,
who first taught me quantum mechanics

Table of Contents

List of Figures

List of Tables

List of Equations

I. Introduction

I.A. Motivation

When an electron is electronically excited to a Rydberg state, it is promoted to an orbital with a high principal quantum number, becoming decoupled from the ion core. It then can be observed how these Rydberg electrons exchange energy and angular momentum with nuclei and how a molecule's rotational, vibrational, and electronic motions interact. Over the years, calcium monofluoride (CaF) has provided spectroscopists with a simple system for studying these intramolecular processes. This diatomic molecule contains two closed-shell ions, Ca^{2+} and F^{-}, and one electron in a Rydberg orbital that is weakly coupled to the core.

Experimentally, two optical transitions are required to excite an electron of CaF into its Rydberg levels (Figure 1). The energy separation between the intracomplex Rydberg orbitals (for instance, between the levels of n*=19 in Figure 1) falls within the THz (10^{12} Hz) frequency range. Because the technique of time-domain terahertz spectroscopy can generate and detect frequencies ranging from about 0.1 to 20 THz (3 to 600 cm^{-1})[1], this technique will to be used to study the transitions between these levels. The principles of time-domain terahertz spectroscopy and the components of the spectrometer that has been built for the experiment will be explained in more detail in the experimental section.

In preparation for the experiments with CaF, the spectrometer will be tested by recording rotational spectra of small polyatomic molecules. As the CaF experiments will require three sources of excitation (triple resonance), it is prudent to start with a simpler

7

n*=19.2 { ——————↑—————— 1.5 cm^{-1} = 0.05 THz

6.6 cm^{-1} = 0.2 THz

n*=19 ————————↑————————

ns   16000 cm^{-1}

D$^2\Sigma^+$ ————————↑————————

ns   30000 cm^{-1}

X$^2\Sigma^+$ ————————↑————————
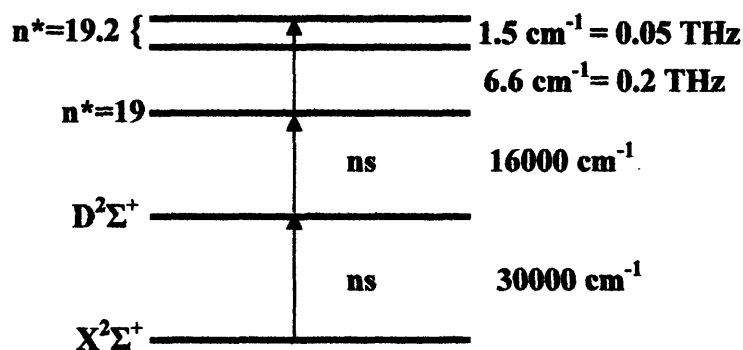
Figure 1 Energy level separations of CaF. The two levels of n*=19.2 have different quantum defects.

experiment that involves recording a rotational spectrum of electronically excited formaldehyde using double resonance. A pulsed dye laser will be used to electronically excite formaldehyde, and the THz electric field will induce pure rotational transitions in both the ground and excited states. It becomes an important task, then, to predict how both the THz electric field and the information it contains about the ground state rotational spectrum are affected when the dye laser is applied. It can be determined which transitions will be visible in the spectrum, based on the frequency of the dye laser, and the strengths associated with those transitions.

I.B. General Method of Calculation

The first step in predicting the double resonance spectrum is to select a single electronic transition, beginning from a level in the electronic-vibrational ground state. Tuning the dye laser to the frequency associated with the electronic transition will remove population from the initial level in the ground state and populate a single level in the excited state. The THz electric field will cause pure rotational transitions in both the ground and excited states, the strengths of which will be proportional to the population differences between the initial and final states of the allowed rotational transitions. In the

ground state, the greatest population differences will be between the depopulated level and its two adjacent J-levels. The populations in the adjacent levels will be transferred into the initial level through stimulated absorption and stimulated emission. In the excited state, the population in the level reached by the electronic transition will be transferred into its two adjacent rotational states, also through absorption and emission. In order to maximize the population differences, electronic excitation should occur from the most populated quantum state, which can be determined from a Boltzmann distribution. Maximizing the population differences should allow the four rotational transitions described above (two absorptions, two emissions) to become the most intense components in the THz spectrum.

The $\tilde{A}\,^1A_2 \leftarrow \tilde{X}\,^1A_1$ electronic transition was chosen for the experiment because it has been thoroughly studied and its band structure and the rotational constants of the two states have been determined. Its frequency range can also be reached by the dye laser. The first spectroscopists to analyze the rotational structure of several bands within this transition were Dieke and Kistiakowsky in 1934.[2] An absorption spectrum of this electronic transition from 250-360 nm is shown in Figure 2. Around 353 nm is the first vibronically allowed transition, the 4^1_0 band. This band, diagramed in Figure 3, corresponds to a vibronic transition for formaldehyde's 4th vibrational mode (out-of-plane bending) from v" = 0 in the ground electronic state ($\tilde{X}\,^1A_1$) to v' = 1 in the first electronically excited state ($\tilde{A}\,^1A_2$). The initial state for electronic excitation will be chosen from this 4^1_0 band because of its intensity and isolation from other bands in the spectrum.
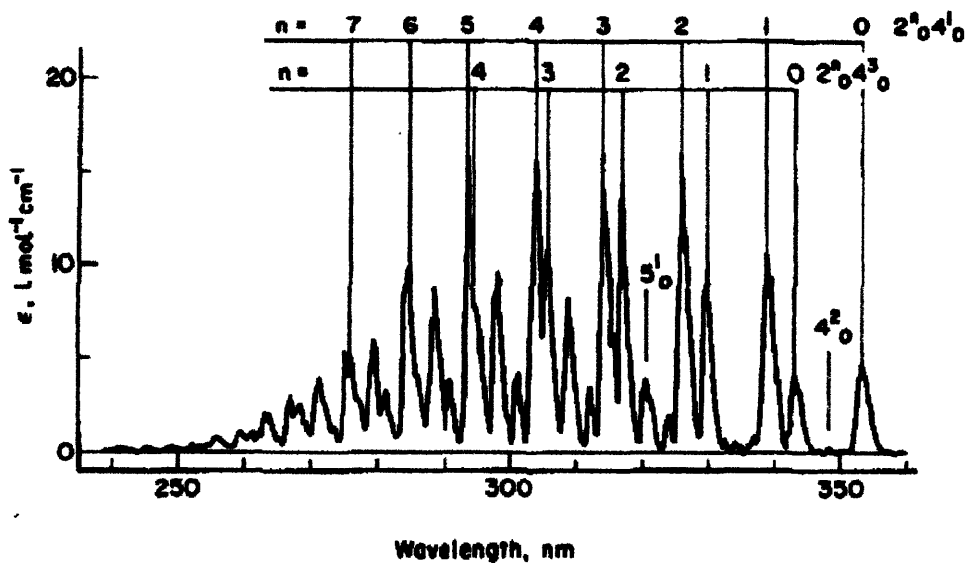
Figure 2 Absorption spectrum of formaldehyde. The band around 353 nm (furthest to the right) corresponds to the 4^1_0 vibronic transition. Figure adapted from Ref. (3).
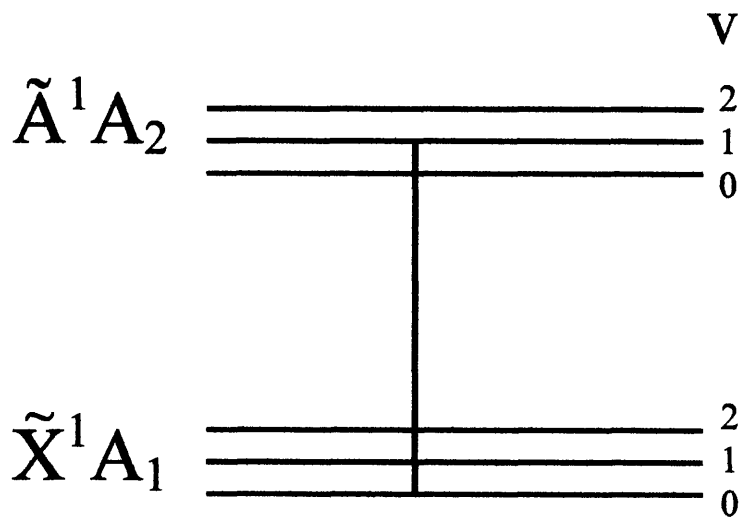
Figure 3 Energy level diagram of the ground and first electronic states of formaldehyde showing the 4^1_0 vibronic transition.

10
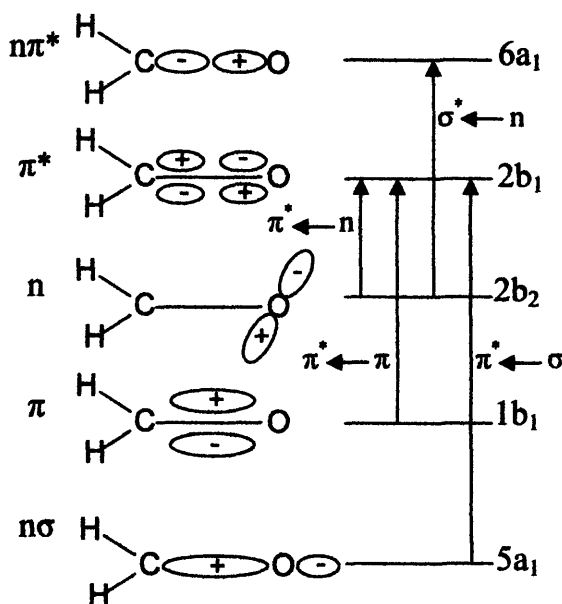
Figure 4 Molecular orbital diagram for the carbonyl of formaldehyde, showing electronic transitions and orbital symmetries. Figure adapted from Ref. (4).

I.C. Group Theory and Selection Rules for Electronic and Pure Rotational Transitions

The $\tilde{A}\ ^1A_2 \leftarrow \tilde{X}\ ^1A_1$ electronic transition involves transferring an electron from a non-bonding orbital on the oxygen atom to an antibonding π^* orbital along the C–O double bond, denoted as an $\pi^* \leftarrow$ n transition.[4] Figure 4 shows a molecular orbital diagram for the carbonyl of formaldehyde that includes the orbital symmetries and the observed electronic transitions. Formaldehyde has six valence electrons with a ground state electron configuration of $(a_1)^2(b_1)^2(b_2)^2$, corresponding to $^1A_1$ symmetry. The $\pi^* \leftarrow$ n transition, as shown by Figure 4, creates a new electron configuration of $(a_1)^2(b_1)^2(b_2)(b_1^*)$, which corresponds to $^1A_2$ symmetry.[5]

In its ground state, formaldehyde belongs to the C_{2v} symmetry group. Examination of its character table (Figure 5) shows that the A_2 irreducible representation does not transform with the x, y, or z axes of the dipole moment vector, meaning that the

C_{2v}	E	C_2	$\sigma(xz)$	$\sigma(yz)$		
A_1	1	1	1	1	z	x^2, y^2, z^2
A_2	1	1	-1	-1	R_z	xy
B_1	1	-1	1	-1	x, R_y	xz
B_2	1	-1	-1	1	y, R_x	yz

Figure 5 C_{2v} character table for formaldehyde

$v_1 (a_1)$
C-H symmetric stretch

$v_2 (a_1)$
C=O stretch

$v_3 (a_1)$
CH$_2$ scissor

$v_4 (b_1)$
out-of-plane bend

$v_5 (b_2)$
C-H stretch

$v_6 (b_2)$
CH$_2$ rock
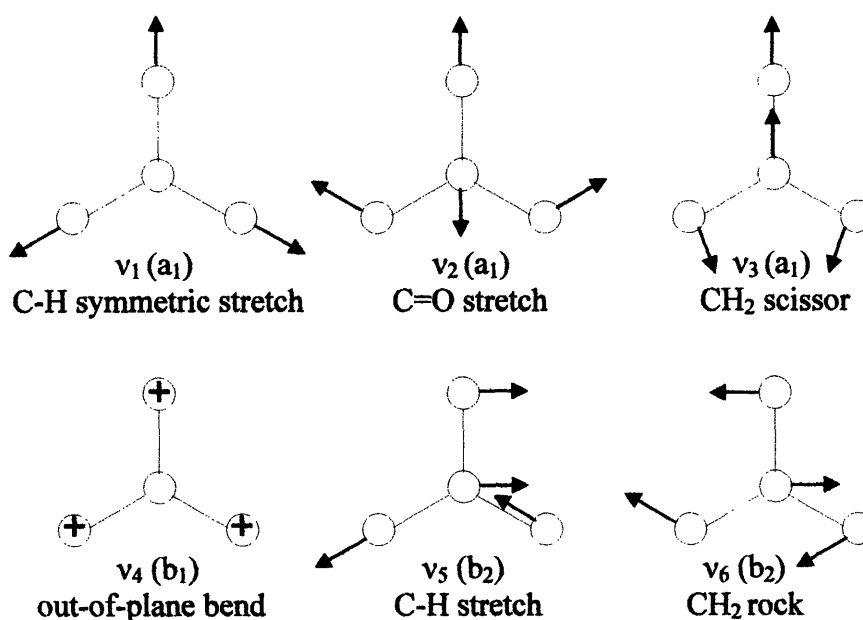
Figure 6 Formaldehyde's six vibrational modes and associated symmetries. '+' refers to the out-of-plane direction. Figure adapted from Ref. (4).

$\tilde{A}\,^1A_2 \leftarrow \tilde{X}\,^1A_1$ transition is electric-dipole forbidden. In order for the transition to occur, it must be accompanied by an odd number of quanta in formaldehyde's fourth vibrational mode (v_4), which corresponds to out-of-plane bending. Figure 6 summarizes formaldehyde's six vibrational modes and their symmetries.

The out-of-plane bending mode has B_1 symmetry. The direct product between the symmetries of the v_4 mode and the final electronic state results in $B_1 \otimes A_2 = B_2$
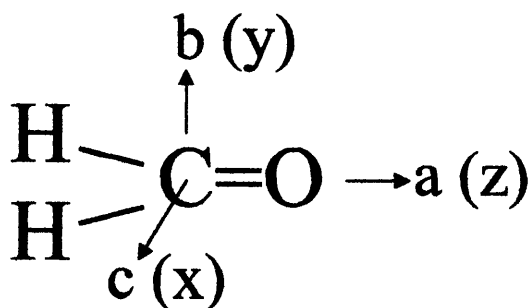
Figure 7 The x(c), y(b), and z(a) axes of formaldehyde.

symmetry, which transforms as formaldehyde's y-axis. Figure 7 shows the labeling

conventions for formaldehyde's three axes. The three Cartesian coordinate axes (x, y,

and z) are defined by the conventions of group theory. The moments of inertia can be

determined about each of these axes, and the a, b, and c labeling convention arises from

$I_a < I_b < I_c.$ The z(a) axis is along the C–O double bond (which is also the symmetry

axis), while the y(b) axis is in the plane of the molecule and perpendicular to the double

bond. The x(c) axis is perpendicular to the page and also to both the y and z axes.

Since the y-axis, with B_2 symmetry, corresponds to the b-axis (which is

perpendicular to the z-axis) electronic transitions will have perpendicular, b-type

selection rules of $\Delta J = 0, \pm 1$ and $\Delta K = \pm 1$. J is the rotational quantum number, and K is

the quantum number for the projection of angular momentum on the symmetry axis of the

molecule. In contrast, the pure rotational spectrum follows a-type selection rules, since

the permanent dipole moment lies along the a(z) axis. The ground state has a dipole

moment of 2.33 D, while the excited state has a dipole moment of 1.56 D.[3] The a-type

selection rules are $\Delta J = \pm 1$ and $\Delta K = 0$.

13

Table 1 Summary of the rotational constants (in cm^{-1}) for the zero-point vibrational levels of the $\tilde{A}\,^1A_2$ and $\tilde{X}\,^1A_1$ electronic states[3].

Rotational constant	$\tilde{X}\,^1A_1$	$\tilde{A}\,^1A_2$
A	9.399019	8.75194
B	1.294535	1.12501
C	1.133407	1.01142

I.D. Formaldehyde as a Prolate Symmetric Top

A polyatomic molecule, formaldehyde has three rotational constants, A, B, and C, associated with the three axes defined in Figure 7. These values change for each electronic and vibrational state. Table 1 summarizes the values for these constants for the zero-point vibrational levels of the ground and first electronic excited states. Since A ≠ B ≠ C, formaldehyde is an asymmetric top. However, in the case that A > B = C, a molecule fits the description of a prolate symmetric top, as can formaldehyde since B≈C. In contrast, if A = B > C, the top is considered an oblate symmetric top. Approximating formaldehyde as a prolate symmetric top greatly simplifies the energy level expressions used in predicting the spectrum. For a prolate symmetric top, the energy of a level is defined by

$$F(J,K) = \overline{B}J(J+1) + (A-\overline{B})K^2 \qquad (I.D.1)$$

where $\overline{B}$ is the average of B and C.

II. Experimental

The development of THz spectroscopy began in the 1980s,[1] making it a relatively new technique for studying the motions of molecules, and its implementation and applications are still evolving. THz, or far-IR, radiation falls between the infrared and microwave regions of the electromagnetic spectrum (Figure 8), and it has been found that various molecular processes operate within this frequency range. Such processes
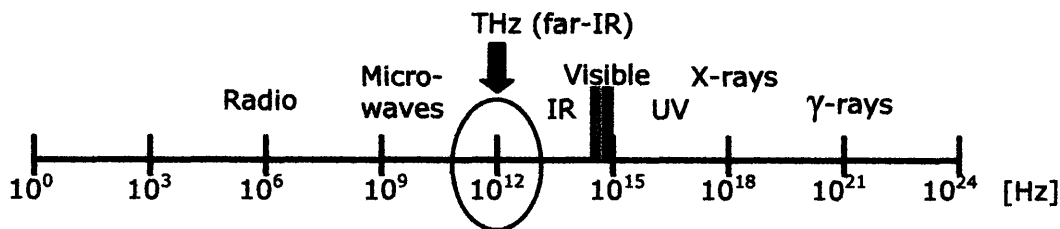
Figure 8 Electro-magnetic spectrum, showing the THz frequency range.

include the collective vibrations of proteins, DNA, and other biomolecules, as well as phonon modes of solids.[1,6] As in the present example, THz radiation can be used for pure rotational spectroscopy in the gas phase. Additional applications include studying the optical properties of semiconductors, electro-optic crystals, and quantum dots as well as three-dimensional imaging of materials, including ceramics and semiconductors.[1,6] THz spectroscopy generally covers a range of 0.1-20 THz.[1]

Combined with electro-optic detection, time-domain THz spectroscopy's main advantage is that it measures a signal proportional to the electric field as it changes with time, preserving both the amplitude and phase of the elements in the spectrum. These pieces of information allow both the absorption coefficient and index of refraction of the sample to be determined without using the Kramers-Kronig relations, a method involving complex analysis. The Kramers-Kronig relations give expressions for the real and imaginary parts of the susceptibility of the system (the susceptibility is a scalar that relates electric field to polarization density), and they must be used if only the intensity, and not the electric field, is measured. The index of refraction depends on the real part of the susceptibility, while the absorption coefficient depends on the imaginary part.[7]

Compared to Kramers-Kronig analysis, THz spectroscopy uses a more direct method to obtain these parameters. The index of refraction and absorption coefficient

can be extracted from the real and imaginary parts of the frequency-dependent complex

transmission coefficient, which is obtained by taking the ratio of the Fourier transforms

of the time-domain THz waveforms recorded with and without the sample present.[8] The

block diagram below illustrates this process:

$$E_S(t) \xrightarrow{\text{Fourier Transform}} E_S(\omega) \xrightarrow{\text{division}} T(\omega) = \frac{E_S(\omega)}{E_0(\omega)} \xrightarrow{\text{Im}} \text{absorption coefficient}$$

$$E_0(t) \xrightarrow{} E_0(\omega) \qquad \xrightarrow{\text{Re}} \text{index of refraction}$$
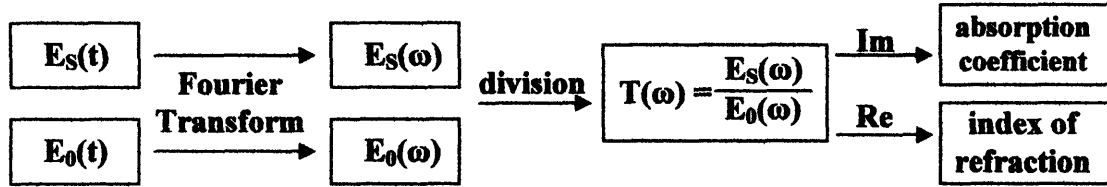
$E_s(t)$ and $E_0(t)$ are the time-dependent THz waveforms modified and unmodified by the

formaldehyde sample, respectively, and $E_s(\omega)$ and $E_0(\omega)$ are their Fourier transforms.

$T(\omega)$ is the complex transmission coefficient.

Figure 9 outlines the geometry of the time-domain THz spectrometer used for the

experiment. An 800 nm pulsed Ti:Sapphire laser beam is first split by a beam splitter

into a pump beam and a probe beam. The pump beam is used for generating the THz

pulses that propagate through and are modified by the sample. The probe beam is used

for detecting the time-dependent THz electric field. The pump beam passes through a

lithium niobate ($LiNbO_3$) crystal, whose surface is oriented perpendicularly to the

incident pump beam. If one thinks of lithium niobate as a collection of anharmonic

oscillators, when the pump beam propagates through the crystal its electric field couples

with the oscillations and, through the nonlinear process of optical rectification, creates a

new electric field with a continuous range of frequencies in the THz range.[9]

After generation, the THz electric field is collimated and focused by two

parabolic mirrors through a stainless steel cell that contains the sample. In the double

resonance experiment, a beam from a pulsed dye laser will also have to travel collinearly
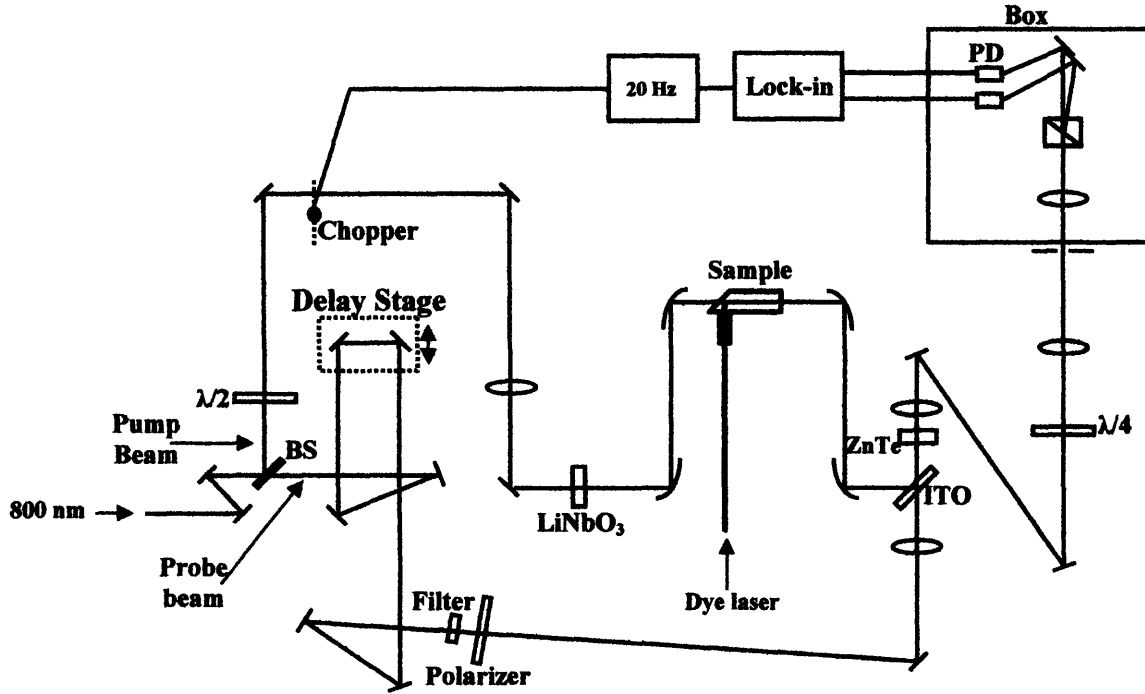
Figure 9 THz spectrometer geometry, showing the pump beam, probe beam, and cell design.

through the cell with the THz electric field in order to maximize the double resonance

signal. To accomplish this, the cell contains a special fixture through which the two

beams enter the cell. The THz electric field enters through a 7mm-thick silicon window

that is set at a 45° angle. The dye laser beam enters through a quartz Brewster window

(at a 33° angle) that is set on a separate arm placed perpendicularly to the main body of

the cell. The arm is positioned so that the dye laser should hit the center of the silicon

window inside the cell. Because the silicon window is polished to reflect optical

wavelengths (with 70% reflectivity), the dye laser beam reflects off of the surface and

copropagates with the THz electric field.

Absorption of the electric field by the sample modifies the THz waveform. Two

more parabolic mirrors refocus and collimate the modified THz radiation onto an ITO

crystal, which reflects the THz electric field. The probe beam, which is near IR, has been propagating along a different path, but it arrives at the ITO and passes through unmodified. The probe beam and the THz electric field then copropagate through a ZnTe crystal. ZnTe is a nonlinear optical material, meaning that an applied electric field will change certain of its properties, such as its index of refraction. By this phenomenon, known as the electro-optic effect, the THz electric field alters the ZnTe crystal's index of refraction, which in turn modifies the polarization of the probe beam. The change in the polarization of the probe beam results in a signal that is proportional to the electric field of the THz signal.

A balanced detection system is used to measure the signal carried by the probe beam. After passing through the ZnTe crystal, a quarter-wave plate circularly polarizes the probe beam. After passing through sample of formaldehyde and the quarter-wave plate, the THz waveform will be composed of two orthogonal, but unequal, components, resulting in an overall ellipsoidal polarization. A Wollaston prism splits the two orthogonal components, and each is sent to a photodiode. A digital lock-in amplifier samples the difference between the intensity of the two components, amplifies the signal, and multiplies it by a reference frequency (20 Hz for the double resonance experiment) that is provided by chopping the pump beam with a chopper wheel. The chopper and digital lock-in amplifier system improve the signal-to-noise ratio by about a factor of 20 compared to an analog lock-in/chopper system. During a scan, the delay stage alters the path length, which is equivalent to the delay, of the probe beam, allowing the balanced detection system to record a signal proportional to the THz electric field as a function of
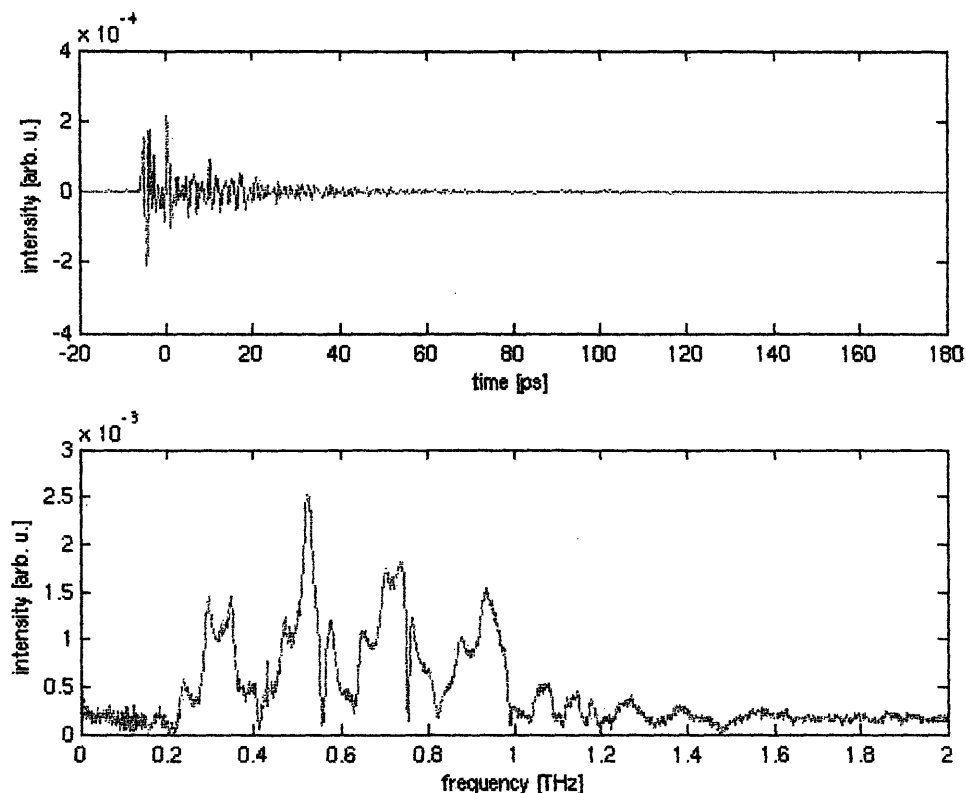
Figure 10 The top graph shows the THz waveform generated in 2.5mm Mg-doped LiNbO₃ as a function of time. The bottom graph is the Fourier transform of the waveform as a function of frequency (THz).

time. A THz waveform, unmodified by the sample and generated in a 2.5mm Mg-doped LiNbO₃ crystal is shown in the top plot of Figure 10. The bottom plot of Figure 10 is the Fourier transform of the waveform, showing the spectral content.

III. Results and Discussion

III.A Selecting an Initial State

The electronic transition should originate from formaldehyde's most populated quantum state in order to maximize the number of molecules excited to the $\tilde{A}\,^1A_2$ level. At room temperature, formaldehyde has a thermal distribution of states according to

$$f_j = \frac{(2J+1)(e^{(-hc\bar{\nu}/kT)})}{\frac{1}{\sigma}\left(\frac{kT}{hc}\right)^{3/2}\sqrt{\frac{\pi c^3}{ABC}}} \qquad \text{(III.A.1)}$$

where f_J represents the fraction of molecules present in each state, $(2J+1)$ is the

degeneracy for a prolate symmetric top, $\bar{\nu}$ is given by the energy level equation of I.D.1,

k is the Boltzmann constant, T is the temperature in Kelvins, c is the speed of light in

cm/s, A, B, and C are the rotational constants found in Table 1, and σ is equal to 2, the

symmetry number of formaldehyde. The denominator of the above equation is the

rotational partition function. The equation was graphed for J = 0 through J = 13, with K

= 0,1,..., J, shown in Figure 11. The most populated state was determined to be J = 9, K =

0, which corresponds to a fractional population of 0.0153.
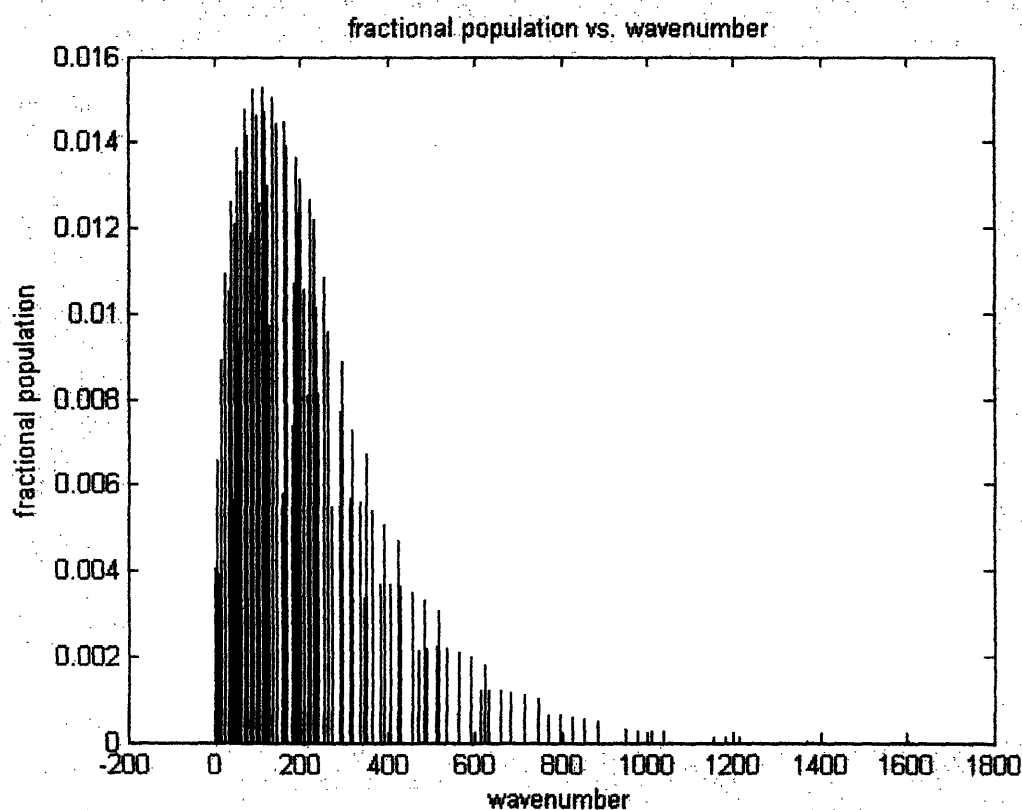
Figure 11 Boltzmann distribution of states at 298 K.

III. B. Choosing an Electronic Transition

Appendix I contains the MATLAB[10] routine "formspectrum.m" that was written to calculate the most populated ground state level. The program then takes the quantum numbers $J = 9$, $K = 0$ and applies the selection rules for perpendicular, b-type electronic transitions presented in section I.C. ($\Delta J = 0, \pm 1$ and $\Delta K = \pm 1$) in order to obtain the rotational structure of the allowed electronic transitions. Since K cannot be negative, applying the selection rules yields three lines in the electronic spectrum corresponding to the rP, rQ, and rR branches. In this notation, "r" denotes $\Delta K = +1$ and "P," "Q," and "R" denote a change in J of -1, 0, and +1, respectively.

The intensities of the lines were calculated according to

$$ I_{KJ} \propto (2J+1)\bar{\nu}_{el}e^{(-hc\bar{\nu}/kT)}A_{KJ} \qquad (III.B.1)^{11} $$

where (2J + 1) is the degeneracy of the initial level (J = 9, K= 0), $\bar{\nu}_{el}$ is the frequency of the electronic transition, and the exponential term is the Boltzmann factor for the initial level. A_{KJ} are the Hönl-London factors:

$$ \text{R branch } (\Delta J = +1) \qquad A_{KJ} = \frac{(J+2\pm K)(J+1\pm K)}{(J+1)(2J+1)} \qquad (III.B.2)^{11} $$

$$ \text{Q branch } (\Delta J = 0) \qquad A_{KJ} = \frac{(J+1\pm K)(J\mp K)}{J(J+1)} \qquad (III.B.3)^{11} $$

$$ \text{P branch } (\Delta J = -1) \qquad A_{KJ} = \frac{(J-1\mp K)(J\mp K)}{J(2J+1)} \qquad (III.B.4)^{11} $$

In these expressions, the upper sign is for $\Delta K = +1$, while the lower is for $\Delta K = -1$.

The frequency of the electronic transitions, $\bar{\nu}_{el}$, can be calculated by summing the ground state energy for J = 9, K= 0 with the energy level separation of the 4^1_0 transition
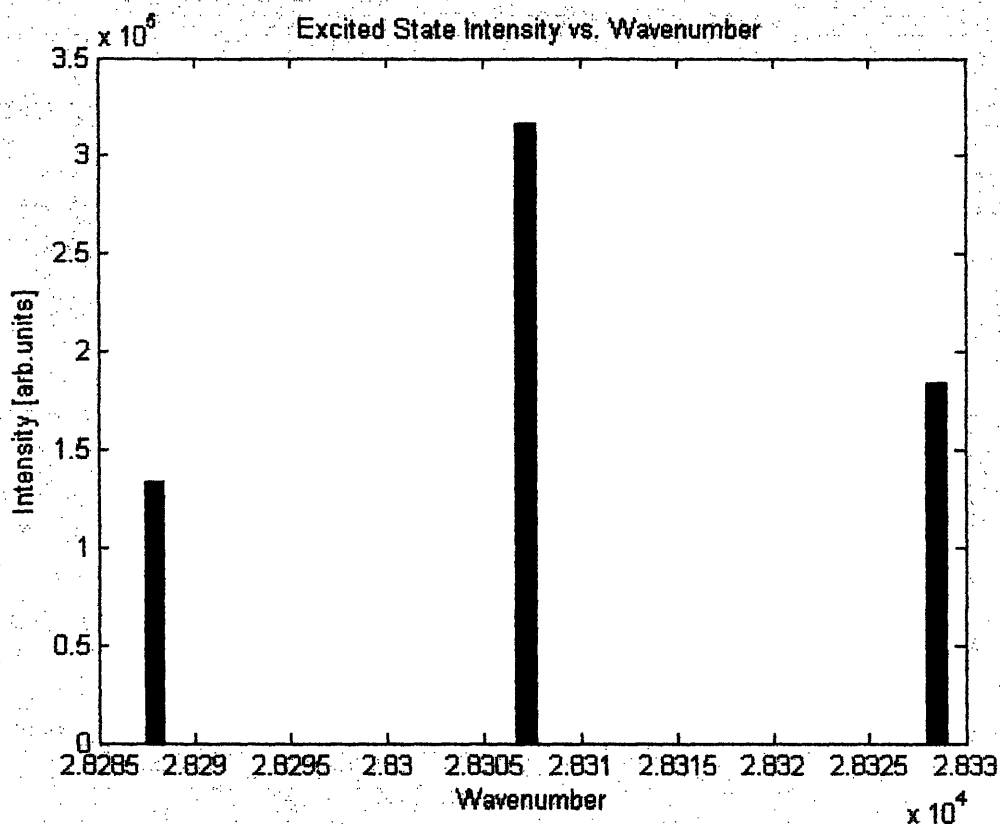
Figure 12 Allowed electronic transitions, showing from left to right, the rP, rQ, and rR lines.

Table 2 Summary of electronic transitions, frequencies, and intensities.

transition	type	frequency (cm^{-1})	Intensity (arb.units) (x 10^5)
$J_{8 \leftarrow 9}$, $K_{1 \leftarrow 0}$	rP	28287.90	1.3345
$J_{9 \leftarrow 9}$, $K_{1 \leftarrow 0}$	rQ	28307.13	3.1715
$J_{10 \leftarrow 9}$, $K_{1 \leftarrow 0}$	rR	28328.49	1.8365

(28312.561 cm^{-1})[3] and subtracting the energy of the excited rotational state. Equation I.D.1 may be used for the energies in the excited state, substituting the ground state rotational constants for those of the excited state.

Figure 12 shows the intensities of the three allowed electronic transitions (rP,rQ, and rR) described above. Table 2 lists the frequencies associated with those transitions. Note that sum of the intensities for the rP and rR transitions equals the intensity for the

rQ transition. The experiment requires one electronic transition (which is followed by pure rotational transitions), so the most intense transition should be selected for pumping by the dye laser. The line with the highest intensity is the rQ branch at 28307.13 cm^{-1} (353.2679 nm), which is the frequency to which the dye laser should be tuned.

III.C. Calculating the Excited State Population

The strengths of the pure rotational lines will depend upon the number of molecules that the dye laser can excite to the $\tilde{A}\ {}^{1}A_2$ state. The fraction of molecules excited from the initial state is calculated by taking the product of the photon flux of the dye laser beam and the absorption cross section of the electronic transition.[12] An absorption cross section is equivalent to the effective area that a molecule presents to a stream of photons, given in units of cm^2. The number of photons is calculated by

$$\Phi = \frac{photons}{pulse \cdot cm^2} = energy\left[\frac{J}{pulse}\right] \div hc\bar{v}_{el}\left[\frac{J}{photon}\right] \div spot\ size\ [cm^2] \qquad (III.C.1)$$

where $\bar{v}_{el}$, in this case, is equal to 28307.13 cm^{-1}, h is Planck's constant, and c is the speed of light in cm/s. The maximum pulse energy delivered by the dye laser is 3 x 10^{-3} J/pulse, and the spot size is 0.0314 cm^2.

The absorption cross section, σ, for a Lorentzian line shape, is given by

$$\sigma = \frac{3.914x10^{-19}\bar{v}|\mu_{ij}|^2}{\Delta\bar{v}} \qquad [cm^2] \qquad (III.C.2)^{13}$$

where

$$\Delta\bar{v} = 7.2x10^{-7}\bar{v}_{el}\sqrt{\frac{T}{M}} \qquad [cm^{-1}] \qquad (III.C.3)^{13}$$

23

with $\bar{\nu}$ and $\left|\mu_{ij}\right|^2$ as the frequency (in wavenumbers) and the square of the transition

dipole moment (in Debye) for the 4^1_0 vibronic transition, respectively. The transition

dipole moment is equal to 0.629×10^{-2} a.u.[14], or 0.0160 Debye. Since formaldehyde has a

relatively long spontaneous lifetime of 100 ns[15], the lines are Doppler broadened rather

than lifetime broadened. The Doppler broadening, given by equation III.B.6., is equal to

0.06 cm^{-1}. T is 298 K, and M is the mass of formaldehyde in atomic mass units (30

a.m.u.). Evaluation of equation III.C.2 yields an absorption cross section of 4.41×10^{-17}

cm^2 for the electronic transition.

As described previously, the fraction of molecules excited from a certain state is

then calculated by

$$\text{Fraction} = \Phi\sigma \qquad \qquad \text{(III.C.4.)}$$

This calculation assumes that stimulated absorption is the only factor populating

the excited state, but stimulated emission must also be included. The transition rate, W,

for stimulated absorption and emission between levels 1 and 2 depends on the energy

density, ρ, of the laser, the number density of each level, N, and a quantity known as the

Einstein B coefficient. The rate of spontaneous decay from level 2 into a ground state

level is given by the Einstein A coefficient. For example, decay from level 2 into level

one corresponds to A_{21}. The rate of spontaneous emission is equal to the sum of all the

Einstein A coefficients for decay from level 2 into each of the ground state levels. This

sum is also equal to $1/\tau_{sp}$, where τ_{sp} is the spontaneous lifetime. For formaldehyde, τ_{sp} is

100 ns.[15] Because this is a relatively long lifetime, the effects of spontaneous emission

can be ignored in the calculation. The Einstein A and B coefficients and their associated

transitions are represented in Figure 13.
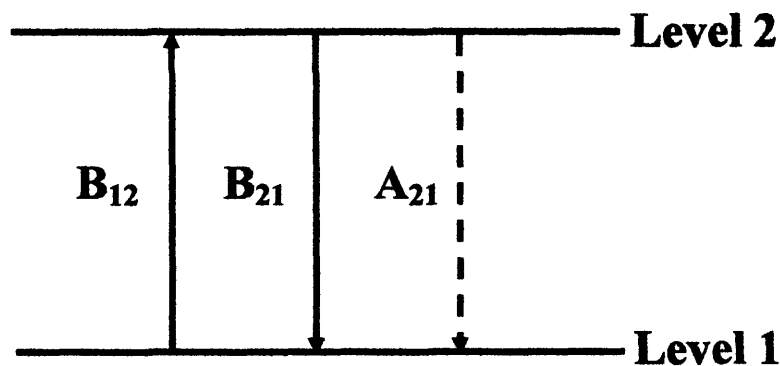
Figure 13 Einstein A and B coefficients.

(stimulated absorption) $W_{12} = B_{12}\rho N_1$ $(III.C.5)^{16}$

(stimulated emission) $W_{21} = B_{21}\rho N_2$ $(III.C.6)^{16}$

(spontaneous emission) $W_{21,sp} = \sum_j A_{2j}N_2$ $(III.C.7)^{16}$

B_{12} and B_{21} are related by the ratio of the degeneracies, g_i, for each level:

$$B_{12} = \frac{g_2}{g_1} B_{21} = \frac{(2J'+1)}{(2J''+1)} B_{21} \qquad (III.C.8)^{16}$$

Since $J' = J'' = 9$ for the electronic transition, the degeneracies of each level are

equal, and $B_{12} = B_{21}$. Because of this relation, half of the molecules that are excited by

the laser move into the excited state while the other half return to the ground state. The

total number density excited from the $J = 9$, $K= 0$ can then be calculated by

$$N_2 = \frac{1}{2} \text{Fraction } f_J N_{total} \qquad (III.C.9)$$

where f_J is the fraction of molecules in the $J = 9$, $K = 0$ state calculated by equation

III.A.1, and N_{total} is the total number density in the cell. For example, at 200 torr, $N_2 =$

25

Fraction Excited out of Initial State vs. Laser Power

Fraction of Molecules Excited Out of the Initial State

0.6
0.5
0.4
0.3
0.2
0.1
0

0   0.5   1   1.5   2   2.5   3

Joules/pulse

x 10^{-3}
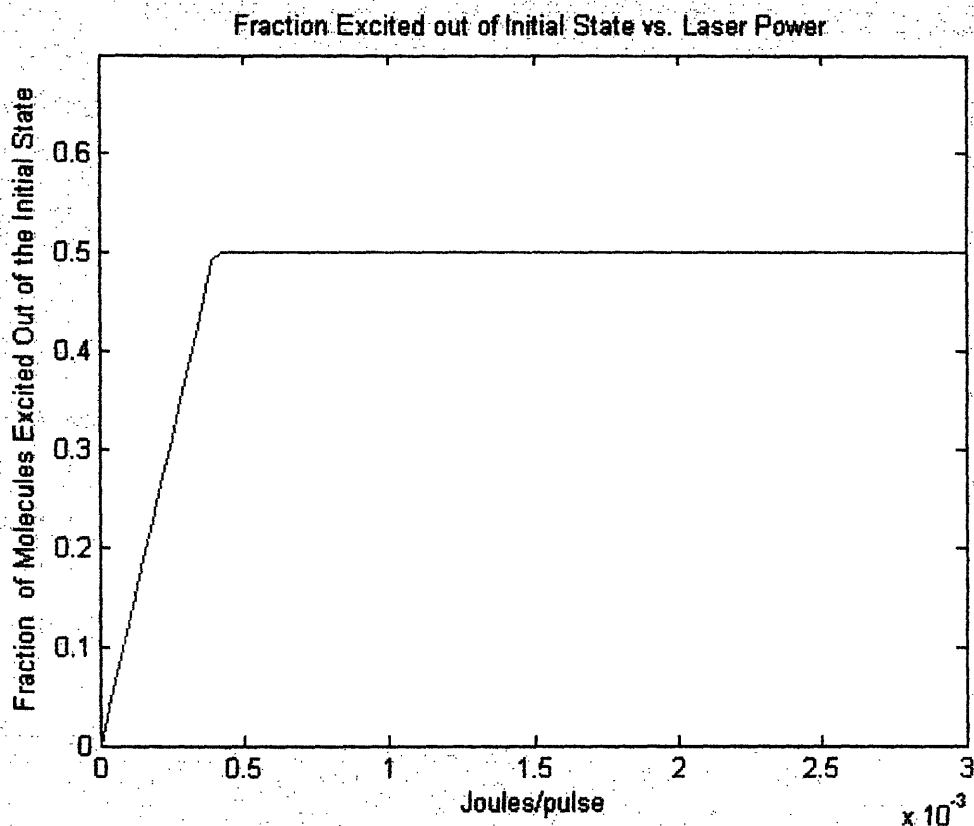
Figure 14 Fraction of molecules excited out of the initial state versus laser power. This fraction, multiplied by N_{total} will yield the population (number density) in the excited state.

4.943 x 10^{16} molecules/cm^3. Dividing equation III.C.10 by f_J and N_{total} gives the overall fraction of molecules excited out of the ground state, which was graphed versus laser power in Figure 14. At 200 torr, N_{total} is equal to 6.465 x 10^{18} molecules/cm^3. Note that saturation occurs around 0.4 mJ/pulse, with 50% of the ground state molecules from J = 9, K= 0 excited to the first electronic state. Appendix II contains the MATLAB routine "ex_pop_plot.m" that was written to calculate the quantities discussed in this section.

III. D. The Pure Rotational Spectrum

If tuned to 28307.13 cm^{-1} (353.2679 nm), the dye laser will transfer half of the molecules in the J = 9, K=0 level in the ground state to the J = 9, K = 1 level in the

excited state (the rQ branch). Addition of THz radiation will cause formaldehyde in its excited and ground levels to undergo pure rotational transitions, for which the selection rules were given in section I.C.. In the excited state, there will be an absorption line corresponding to $J_{10\leftarrow 9, K=1}$, and an emission line corresponding to $J_{8\leftarrow 9, K=1}$. In the ground state, there will be absorption line, $J_{9\leftarrow 8, K=0}$, and an emission line, $J_{9\leftarrow 10, K=0}$, which serve to repopulate the J = 9, K = 0 state. It will be shown that the strengths of the transitions among the thermally populated levels will be weaker than the four transitions discussed above, which involve larger population differences.

The strength of the lines were calculated in terms of absorption coefficient, α, which is a measure of how much energy a certain population absorbs at a specified frequency, given in units of cm^{-1} (to be distinguished from wavenumbers). The absorption coefficient is equal to the absorption cross section times the population difference between the two levels:

$$\alpha = \sigma(N_1 - N_2) \qquad\qquad \text{(III.D.1)}^4$$

Removing half of the J = 9, K = 0 population and populating the excited state significantly increases the population differences for the $J_{10\leftarrow 9, K=1}$, $J_{8\leftarrow 9, K=1}$, $J_{9\leftarrow 10, K=0}$, and $J_{9\leftarrow 8, K=0}$ transitions. It is assumed that J = 10, K=1, and J = 8, K = 1 in the excited state are initially unpopulated.

In order to use equation III.D.1 to calculate the absorption coefficient for these transitions, the population differences and absorption cross sections for the transitions must be calculated first. Since only the J = 9, K = 1 level is populated in the excited state, the population difference for its transitions will be equal to the number of excited molecules, given by equation III.C.9.

27

The new population differences after excitation for the rotational transitions in the ground state can be calculated by

$$\Delta N_{new} = \left(f_{J',K'} - f_{J'',K''}(1 - \frac{1}{2}\text{fraction}) \right) N_{total} \qquad \text{(III.D.2)}$$

For the absorption cross section, equation III.C.2 may be used again:

$$\sigma = \frac{2.652x10^{-19}\,\bar{\nu}|\mu_{ij}|^2}{\Delta\bar{\nu}} \qquad \text{(III.D.3)}[13]$$

where

$$\Delta\bar{\nu} = \left[10\frac{\text{MHz}}{\text{torr}} \right]\left[\frac{1}{30000\,\text{MHz/cm}^{-1}} \right]P \qquad \text{(III.D.4)}[13]$$

is the term for collision broadening. 10 MHz/torr is an approximation that spectroscopists generally use to estimate collision broadening. P is the pressure of the system in torr. The term $\bar{\nu}$ in equation III.D.3 is the frequency of the rotational transition: $2\bar{B}J''$ for emission, and $2\bar{B}(J''+1)$ for absorption, where $\bar{B}$ is the average of the B and C rotational constants. The square of the transition dipole moment, $|\mu_{ij}|^2$, depends on the square of the permanent dipole moment, μ^2, and a Hönl-London factor for a-type rotational transitions.

$$\text{For absorption, } J+1\leftarrow J: \quad |\mu_{ij}|^2 = \mu^2\frac{(J+1)^2 - K^2}{(J+1)(2J+1)} \qquad \text{(III.D.5)}[17]$$

$$\text{For emission: } J-1\leftarrow J: \quad |\mu_{ij}|^2 = \mu^2\frac{(J^2 - K^2)}{J(2J+1)} \qquad \text{(III.D.6)}[17]$$

As stated before, μ is 2.33 D for the ground state, and 1.56 D for the excited state.[3] The MATLAB routine "rotspec.m" (Appendix III) was written to calculate the values described above, and the results are summarized in Table 3 for a sample pressure of 200

torr. Note that the absorption coefficients for the excited state are weaker than for those for the ground state. Since the frequencies only differ by a few wavenumbers and the population differences are roughly equal to each other, the one factor that significantly affects the absorption coefficient is the square of the transition dipole moment, which is smaller in the excited state.

To determine whether these absorption coefficients have increased compared to those of the other ground state rotational transitions, the initial absorption coefficients (before electronic excitation) can be calculated and compared with the results in Table 3. The initial population differences for the ground state transitions were calculated using the Boltzmann distribution of equation III.A.1:

$$\Delta N_{initial} = (f_{J''} - f_{J'})N_{total} \tag{III.D.7}$$

Since the frequencies do not change, the absorption cross sections of Table 3 can still be used. Table 4 summarizes the results of these calculations for the initial states. Both initial absorption coefficients are weaker by about a factor of 10 than the ones calculated for the new population differences, so electronic excitation should produce four lines much stronger than the thermal ground state rotational spectrum. The four lines and their strengths are plotted in Figure 15, with the rest of the ground state rotational spectrum subtracted out.

Table 3 Summary of results from "rotspec.m", giving the transitions, frequencies, absorption cross sections, and absorption coefficients for the four transitions (at 200 torr).

transition	frequency	population difference (molecules/cm^3)	absorption cross section (cm^2)	absorption coefficient (cm^{-1})
$J_{10\leftarrow 9}$, K=1 (excited)	21.3643 cm^{-1} (0.6409 THz)	4.943 x 10^{16}	1.59 x10^{-17}	7.86
$J_{8\leftarrow 9}$, K=1 (excited)	19.2287 cm^{-1} (0.5769 THz)	4.943 x 10^{16}	1.29 x10^{-17}	6.35
$J_{9\leftarrow 10}$, K= 0 (ground)	24.2794 cm^{-1} (0.7284 THz)	4.774 x 10^{16}	1.19 x10^{-16}	17.6
$J_{9\leftarrow 8}$, K=0 (ground)	21.8515 cm^{-1} (0.6555 THz)	4.888 x 10^{16}	1.32 x10^{-16}	18.0

Table 4 Summary of initial population differences and absorption coefficients before excitation (at 200 torr).

transition	frequency	$\Delta N_{initial}$ (molecules/cm^3)	absorption cross section (cm^2)	initial absorption coefficient (cm^2)
$J_{9\leftarrow 10}$, K= 0 (ground)	24.2794 cm^{-1} (0.7284 THz)	1.649 x 10^{15}	1.19 x10^{-16}	0.642
$J_{9\leftarrow 8}$, K=0 (ground)	21.8515 cm^{-1} (0.6555 THz)	5.500 x 10^{14}	1.32 x10^{-16}	0.203

III.E. Modification of the THz Electric Field

Experimentally, the absorption coefficients calculated in the previous section will

be extracted from the complex transmission coefficient, T(ω), discussed in the

experimental section. In reality, the spectrometer measures the THz electric field, so it is

wise to consider how the signal will change as the electric field travels through the

sample of formaldehyde. Figure 16 shows a simplified diagram of the cell containing

gaseous formaldehyde. The derivations in this section ignore the thickness of the

windows covering the cell, as well as the reflections from those windows. The THz

electric field, propagating to the right, enters through window 1, propagates a distance *d*
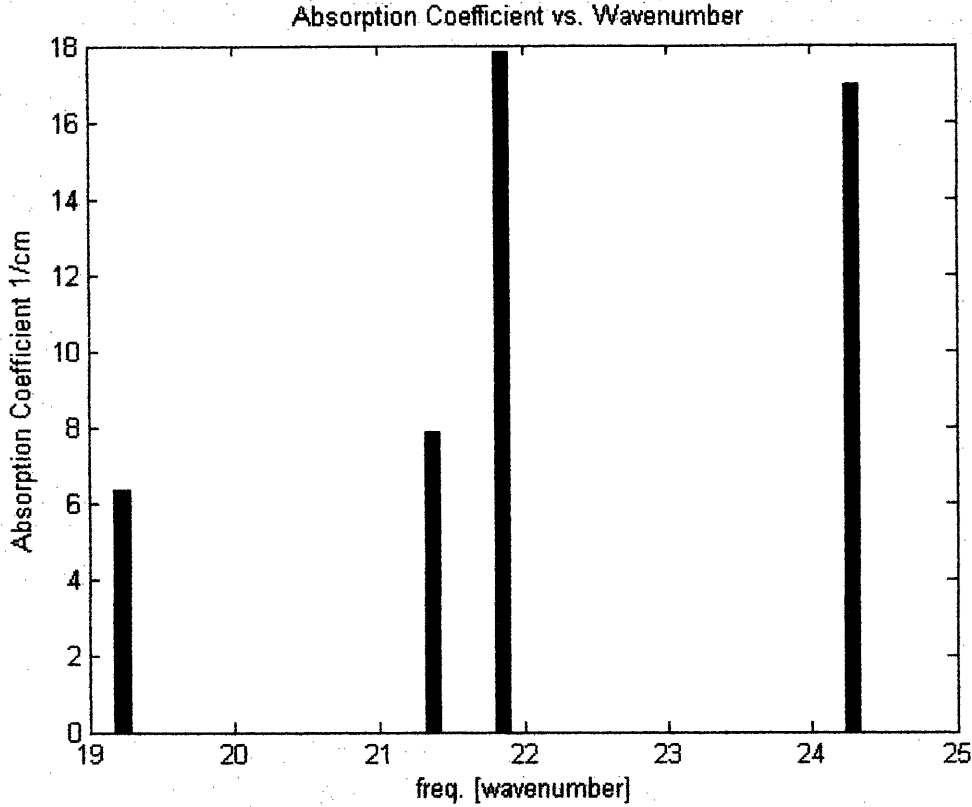
Figure 15 Rotational spectrum. From left to right are the following transitions: $J_{8\leftarrow9,K=1}$, $J_{10\leftarrow9,K=1}$, $J_{8\leftarrow9,K=0}$, and $J_{9\leftarrow10,K=0}$. The absorption coefficients for $J_{8\leftarrow9,K=0}$ and $J_{9\leftarrow10,K=0}$ and all the other ground state rotational transitions for a thermal population have been subtracted.
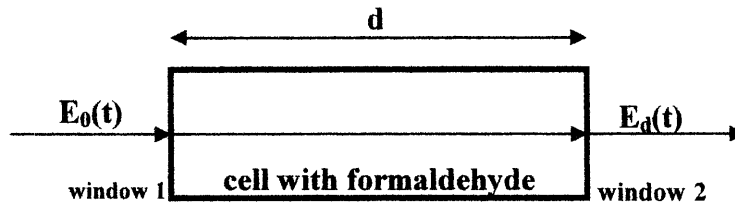
Figure 16 Diagram of cell with incoming and outgoing THz electric fields.

through the cell filled with formaldehyde, and leaves via window 2. The electric field

before entering the cell is denoted as $E_0(t)$, and the field after exiting the cell is $E_d(t)$. In

the absence of sample, $E_0(t)$ will remain unchanged. The time-dependent electric field is

converted to the frequency domain by taking a Fourier transform:

$$E_0(\omega) = \int E_0(t)\exp(-i2\pi\omega\, t)dt \qquad\qquad \text{(III.E.1)}$$

The Fourier transform of the electric field after propagating through the cell will be equal to:

$$E_d(\omega, d) = P(\omega, d)E_0(\omega) \qquad\qquad \text{(III.E.2)}$$

where $P(\omega,d)$ is the propagation coefficient for the medium (formaldehyde) over the cell length, d. The propagation coefficient depends on the medium's complex index of refraction, which serves to modify the waveform as it passes through the medium.

$$P(\omega, d) = \exp\left[-i\frac{\tilde{n}\omega\, d}{c}\right] \qquad\qquad \text{(III.E.3)}[8]$$

where

$$\tilde{n} = n - i\kappa \qquad\qquad \text{(III.E.4)}[8]$$

is the complex index of refraction. The refractive index n and the extinction coefficient κ are both frequency-dependent. The extinction coefficient is related to the absorption coefficient by

$$\alpha = \frac{2\omega\kappa}{c} \qquad\qquad \text{(III.E.5)}$$

Solving equation III.E.5 for the extinction coefficient yields $\kappa = c\alpha/2\omega$. Substituting this and equation III.E.4 into the expression for the propagation constant (equation III.E.3) gives

$$P(\omega, d) = \exp\left[-\frac{in\omega d}{c} - \frac{\alpha d}{2}\right] \qquad\qquad \text{(III.E.6)}$$

According to this equation, the imaginary part of the propagation coefficient, containing the index of refraction, creates an oscillating function that affects the phase of the electric field. The real part of the propagation coefficient, dependent on the

32

absorption coefficient, serves to attenuate the electric field much like the Lambert-Beer Law.

In a non-double resonance experiment, the transmission coefficient will be equal to the ratio of the Fourier transforms of the electric fields recorded with and without the sample present. In the double resonance experiment, however, the transmission coefficient will be the ratio of the Fourier transforms of the electric field recorded with and without applying the dye laser to the formaldehyde sample. These electric fields will be equal to

$$E_1(\omega, d) = P_1(\omega, d)E_0(\omega) = \exp\left[-\frac{in\omega d}{c} - \frac{\alpha_1 d}{2}\right]E_0(\omega) \qquad (III.E.7)$$

for the electric field propagating through the sample without the dye laser

and

$$E_2(\omega, d) = P_2(\omega, d)E_0(\omega) = \exp\left[-\frac{in\omega d}{c} - \frac{\alpha_2 d}{2}\right]E_0(\omega) \qquad (III.E.8)$$

for the electric field propagating through the sample with the dye laser applied, where α_1 and α_2 are the absorption coefficients produced in each situation.
Taking their ratio yields

$$\frac{E_2(\omega, d)}{E_1(\omega, d)} = \exp\left[-(\alpha_2 - \alpha_1)\frac{d}{2}\right] \qquad (III.E.9)$$

Equation III.E.8 demonstrates how the transitions in the ground state which are not affected by the new population differences may be subtracted from the spectrum. If the population difference for a transition does not change in either situation (dye laser or no dye laser), then neither will the absorption coefficient for the transition, making the difference in equation III.E.8 equal to 0 (with a ratio of electric fields equal to 1). For the

33

four transitions discussed in section III.D, the absorption coefficients will change, making the difference in absorption coefficients non-zero. Figure 15 shows these $\alpha_2 - \alpha_1$ differences.

IV. Conclusions

The model presented here predicts that four rotational lines corresponding to $J_{9\leftarrow 8, K=0}$ and $J_{9\leftarrow 10, K=0}$ in the ground state, and $J_{10\leftarrow 9, K=1}$ and $J_{8\leftarrow 9, K=1}$ in the excited state will have absorption coefficient strengths about 10 times larger than those for a ground state rotational spectrum unaffected by the dye laser excitation. This prediction comes from the argument that electronic excitation will increase the population differences between the levels associated with those four transitions, thereby increasing their respective absorption coefficients. Since the absorption coefficients corresponding to other transitions in the ground state do not change, they may be subtracted from the spectrum, leaving those four lines visible in the THz spectrum.

Since this model is not treated with time-dependent quantum mechanics, the system is best approximated as following the Lambert-Beer Law, with formaldehyde removing and donating energy to the electric field via absorption and emission. Using time-dependent quantum mechanics would more accurately predict how the molecules interact with the electro-magnetic fields in the experiment, allowing more accuracy in predicting the changes to the THz waveform. The energy level calculations to predict the transition frequencies, however, should not be affected by this non-rigorous treatment. Since formaldehyde was approximated as a prolate symmetric top when it is really asymmetric, one could theoretically correct the rotational energies using perturbation theory, as described by Dieke and Kistiakowsky.[2]

A benefit of this model is its flexibility in case that certain parameters must be changed. For instance, if the dye laser cannot produce enough energy to excite half of the molecules out of the initial state, one can use Figure 14 to select the appropriate fraction for recalculating the excited state population. A pressure of 200 torr was used as an example pressure for the calculations, but this value can be changed in the codes in order to recalculate the number density of the system. Electronic transitions in the 4^1_0 band beginning from states other than J=9, K=0 may also be studied by changing the values for J" and K" in lines 60 and 61 in "formspec.m." In the event that another vibronic transition is to be studied in the experiment, the rotational constants in the program "formspectrum.m" can be changed easily, and a new electronic transition can be selected. The remaining codes can be altered to account for these changes.

Upcoming work with the experiment involves synthesizing formaldehyde and recording the actual double resonance spectrum with the THz spectrometer. An appropriate dye must also be selected beforehand in order to produce the wavelength around 353 nm that is needed for electronic excitation.

V. References

1. Beard, M.C.; Turner, G.M.; Schmuttenmaer, C.A. J. Phys. Chem. B 2002, 106, 7146-7159.
2. Dieke, G.H.; Kistiakowsky, G.B. *Physical Review* **1934**, 45, 4-28.
3. Clouthier, D.J.; Ramsay, D.A. *Ann. Rev. Phys. Chem.* **1983**, 34, 31-58.
4. Bernath, P.F. *Spectra of Atoms and Molecules*; Oxford University Press: New York, 1995.
5. Moule, D.C.; Walsh, A.D. *Chemical Reviews* **1975**, 75(1), 67-84.
6. Ferguson, B.; Zhang, X.-C. *Nature Materials* **2002**, 1, 26-33.
7. Saleh, B.E.A.; Teich, M.C. *Fundamentals of Photonics*; John Wiley & Sons, Inc.: New York, 1991.
8. Duvillaret, L.; Garet, F.; Coutaz, J.-L. *IEEE Journal of Selected Topics in Quantum Electronics* **1996**, 2(3), 739-746.
9. Shen, Y.R. *The Principles of Nonlinear Optics*; John Wiley & Sons, Inc.: New Jersey, 2003.
10. MATLAB 6.5 The Mathworks, Inc. June 12, 2002.
11. Herzberg, G. *Molecular Spectra and Molecular Structure, vol. III. Electronic Spectra and Electronic Structure of Polyatomic Molecules;* Krieger Publishing Company: Florida, 1991.
12. Duan, Z. "Spectroscopic Study of the Acetylene Species." Ph.D./M.S. thesis. MIT 13 Jan. 2003.
13. Lefebvre-Brion, H.; Field, R.W. *The Spectra and Dynamics of Diatomic Molecules*; Elsevier: The Netherlands, 2004.
14. van Dijk, J.M.F.; Kemper, M.J.H.; Kerp, J.H.M.; Buck, H.M. *J. Chem. Phys.* **1978** 69, 2453-2461.
15. Moore, C.B. *Ann. Rev. Phys. Chem.* **1983**, 34, 525-555.
16. Hilborn, R.C. *Am. J. Phys.* **1982**, 50, 982-986. (corrected version, Feb. 2002)
17. Townes, C.H.; Schawlow, A.L. *Microwave Spectroscopy*; Dover: New York, 1975.

Appendix I: "formspectrum.m"

```
%Program to simulate a double-resonance spectrum of formaldehyde


clear all
close all

%first need rotational partition function, qrot
T = 298.15; %room temperature
A = 9.399019; %rotational constant (cm-1)
b= 1.294535;  %rotational constant (cm-1)
C= 1.133407; %rotational constant (cm-1)
B=(b+C)/2; %average of B and C (for symmetric top approximation)
h = 6.63e-34; %Planck's constant
c = 3e10; %speed of light (cm/s)
Kb= 1.38e-23; %Boltzmann constant

  TrotA = h*c*A/Kb; %rotational temperature, A
  TrotB = h*c*B/Kb; %rotational temperature, B
  TrotC = h*c*C/Kb; %rotational temperature, C
  s = 2; %symmetry number
qrot = ((pi^0.5)/s)*((298^3)/(TrotA*TrotB*TrotC))^0.5; %rotational
partition function

%Now calculate the distribution of states in the v4 mode before
excitation
v_vector=[];      % to allocate space for frequencies
f_J=[];           % to allocate space for populations
J_matrix=[];
K_matrix=[];
f_J_vector=[];

for J = 0:13;
    K = [0:J];
    J_matrix(end+1:end+J+1,1) = J*ones(length(K),1);
    K_matrix(end+1:end+J+1,1) = K';
    v = B*J*(J+1) + (A-B)*K.^2;   %energy for prolate symmetric top
    v_vector(end+1:end+J+1) = v; %defines frequencies for each state
    f_J= (2*J+1)*exp(-h*c*v/(Kb*T))/qrot;
    f_J_vector(end+1:end+J+1) = (2*J+1)*exp(-h*c*v/(Kb*T))/qrot;
end

subplot(2,1,1), bar(v_vector,f_J_vector)
xlabel('wavenumber')
ylabel('fractional population')
title('fractional population vs. wavenumber')

[maxf_J,index_J] = max(f_J_vector);
Jmax=J_matrix(index_J)    %Jmax = 9
Kmax=K_matrix(index_J)    %Kmax = 0
Vn= B*Jmax*(Jmax+1) + (A-B)*Kmax.^2
f_Jtest = (2*Jmax+1)*exp(-h*c*Vn/(Kb*T))/qrot   %makes sure that
calculated Jmax and Kmax return highest fractional population
All = [J_matrix K_matrix f_J_vector'];
```

```
%%now predict rotational structure of electronic transition

%rotational constants for excited state transition, Clouthier
Aex = 8.75194; %rotational constant (cm-1)
bex= 1.12501;  %rotational constant (cm-1)
Cex= 1.01142; %rotational constant (cm-1)
Bex=(bex+Cex)/2; %average of B and C (for symmetric top approximation)


q = 9;  %Jmax   (allows these to be changed to find new lines)
d = 0;  %Kmax   (Kmax should stay 0)


V= B*q*(q+1) + (A-B)*d.^2;  %gives frequency associated with Jmax, Kmax
   Jex = [q-1 q q+1];        %allowed J transitions (delJ=+/-1,0)
   Kex = [d+1 d+1 d+1];      % allowed K transitions (delK=+1) since
Kmax=0
vex = Bex.*Jex.*(Jex + 1) + (Aex-Bex).*Kex.^2;   %excited state energy


   o3_vector = ones(1,3);
   T_o = 28312.561.*o3_vector; %To in cm-1, taken from Ann. Rev. article
(353nm = 28329 cm-1)
   vg = V.*o3_vector; %frequency of J=9,K=0 in ground state in cm-1
vtot = T_o + vex - vg;  %frequency of electronic transition


   v_lower = B*q*(q+1) + (A-B)*d^2; %lower state energy of Jmax, Kmax
boltz = exp(-h*c*v_lower/(Kb*T)); %boltzmann factor for intensity
calculation

%define Honl-London Factors (Akj) for perpendicular transitions (b-type
along plane of hydrogens)
%selection rules delJ=+/-1,0 and delK=+1 (since Kmax=0)

   ArP = (q-1-d)*(q-d)/(q*(2*q+1));
   ArQ = (q+1+d)*(q-d)/(q*(q+1));
   ArR = (q+2+d)*(q+1+d)/((q+1)*(2*q+1));

Akj = [ArP ArQ ArR];

%calculate intensities
g_q = 2*q+1;
Ikj = g_q*Akj*exp(-h*c*V/(Kb*T)).*vtot; %from Herzberg

[maxIkj,index_Jex] = max(Ikj);
y=Jex(index_Jex)    %gives J with highest intensity
z=Kex(index_Jex)    %gives K with highest intensity
w=vtot(index_Jex)   %gives frequency associated with Jmax, Kmax
dye_frequency = 1/w/100*1e9  %gives frequency at which we should set
the dye laser

subplot(2,1,2),
bar(vtot, Ikj,0.05)
xlabel('Wavenumber')
ylabel('Intensity [arb.units]')
title('Excited State Intensity vs. Wavenumber')

data = [Jex' Kex' vtot' Ikj']
```

Appendix II: "ex_pop_plot.m"

```
%Calculate number of molecules in excited state and graph versus laser
%power

clear all
close all

%Calculate absorption cross section using equations from Bob's book
  T=298.15;
  Kb=1.38e-23;
  To = 28312.561;    %41o transition frequency, wavenumbers
  Uij = 0.0160; %from J. Chem. Phys. 69, 2453 (1978), in units of Debye
  w = 28307.13;  %frequency of dye laser
  M = 30; % mass of formaldehyde (amu)
  deltaV = 7.2e-7.*w.*sqrt(T/M)   %Doppler broadening (p.352)
abs_cross = 3.914e-19.*To.*(Uij^2)./deltaV   %peak absorption cross
section in units of cm^2, for Lorentzian lineshape

%Calculate number density in cell
  P = 200; %pressure in torr
Ntotal = 133*P/(Kb*T)/(100^3)   %number density in molecules/cm^3

%Now excited state population, using "fraction" from Richard Duan's
thesis
  energy_pulse = linspace(0,3e-3); %J/pulse
  %rep = 20; %pulses/sec (not actually needed)
   h = 6.63e-34; %Planck's constant
  c = 3e10; %speed of light cm/s
  radius = 1e-3; %radius of dye laser beam
  spotsize = 100^2*pi*radius^2;   %area of beam in cm^2

  f_J = 0.015292;   %fraction of molecules in J=9, K=0 state

  energy_pulse = linspace(0,3e-3);
  photons = energy_pulse./(h*c*w)./spotsize;
fraction = photons.*abs_cross;   %fraction of molecules excited

[y,index] = find(fraction >=1);
fraction(index) = 1;        %replaces all fractions >=1 with 1

N_ex = (1/2).*fraction;  %plots fraction in excited state, multiply by
f_J*Ntotal for number density

plot(energy_pulse, N_ex)
xlabel('Joules/pulse')
ylabel('Fraction  of Molecules Excited Out of the Initial State')
title('Fraction Excited out of Initial State vs. Laser Power')

data = [energy_pulse' N_ex'];
```

Appendix III: "rotspec.m"

```
%Program to calculate the absorption cross sections and absorption
%coefficients associated with the pure rotational transitions in the
ground
%and excited states of formaldehyde after electronic excitation

clear all
close all

%rotational constants for ground state
b= 1.294535;  %rotational constant (cm-1)
C= 1.133407; %rotational constant (cm-1)
B=(b+C)/2; %average of B and C (for symmetric top approximation)

%rotational constants for excited state
bex= 1.12501;  %rotational constant (cm-1)
Cex= 1.01142; %rotational constant (cm-1)
Bex=(bex+Cex)/2; %average of B and C (for symmetric top approximation)

%transition quantum numbers
Qex = [10 9];
Qgr = [10 9];    %rotational quantum number for frequency calculation
                 %Qex:  10 - absorption from J=9,K=1 to J=10 in
excited state
                 %          9 - emission from J=9,K=1 to J=8
                 %                    in excited state
                 %Qgr:  10 - emission from J =10,K=0 to
                 %                    J=9,K=0 in ground state
                 %          9 - absoprtion from J=8, K=0 to J=9 in
ground state

v = [2*Bex.*Qex 2*B.*Qgr];

Uij_ex = 1.56;  %excited state permanent dipole moment in Debye
Uij_gr = 2.33;  %ground state permanent dipole moment in Debye

%rotational transition dipole moments
U1 = Uij_ex^2*((9+1)^2 - 1^2)/((9+1)*(2*9+1));
U2 = Uij_ex^2*(9^2 - 1^2)/(9*(2*9+1));
U3 = Uij_gr^2*(10^2 - 0^2)/(10*(2*10+1));
U4 = Uij_gr^2*((8+1)^2 - 0^2)/((8+1)*(2*8+1));

U = [U1 U2 U3 U4];

P = 200;      %pressure in torr
deltaV = 10/30000*P;  %collison broadening for rotational lines  ,
Bob's book p.352

abs_cross = 3.914e-19.*v.*U./deltaV;

pop_ground_initial = [0 0 1.694e15 5.500e14];   %population differences
for thermal distribution

alpha_initial = abs_cross.*pop_ground_initial  %gives initial alphas in
ground state
```

```
new_pop_diff = [4.9431e16 4.9431e16  4.7737e16 4.8882e16];

alpha_new = abs_cross.*new_pop_diff;

alpha_plot = alpha_new-alpha_initial; %subtracts absorption
coefficients from thermal population transitions

bar(v, alpha_plot, 0.2)
xlabel('freq. [wavenumber]')
ylabel('Absorption Coefficient 1/cm')
title('Absorption Coefficient vs. Wavenumber')

data = [v' new_pop_diff' abs_cross' alpha_new']
```

Acknowledgements

I have quite a few people to thank for helping me complete this thesis. All of the members of the Field Group contributed either insight or moral support along the way (often both), and they have made my undergraduate research experience both rewarding and highly memorable. I must first thank Vladimir Petrović for being my mentor over the past year and half. We have put up with broken vacuum pumps, misaligned mirrors, recalcitrant boxcars, and truant SDGs that go missing for a month, and yet we somehow manage to find a solution. I wish him the best of luck with CaF once I graduate. I cannot thank Professor Bob Field enough for being a wonderful UROP supervisor to work for, patient when answering all my questions and extremely supportive throughout my work here at MIT. My academic advisor, Cathy Drennan, has also provided me with sage counsel for the past four years.

Adam Steeves has repeatedly offered crucial gems of advice, and I appreciate all the help he has given me. Jeff Kay and Bryan Lynch were helpful in hashing out the beginning stages of my predictive model, and I could not have progressed further without their insight. Bryan Matthew Wong and Kyle Bittinger provided me with indispensable help with my MATLAB codes. Wilton Virgo never walks by without saying some words of encouragement. And I can always turn to Sam Lipoff for any type of information, be it absorption cross sections or how to prepare chocolate.

I also want to thank Hans and Kate Bechtel for being the amazing people that they are. Hans has led the way in promoting group bonding experiences, such as movie nights, bowling, and outings to local restaurants, and he and Kate have helped me cope with the insanity of the graduate school process.

Ed Udas, the machinist for the Chemistry Department, has taught me so much, including that even when you mess something up, you can find a way to fix it.

The love and support from those who know me outside of the laboratory must be acknowledged: Kenneth Wu, especially, for providing necessary doses of insanity late at night and pretty much any other hour in the day, and also for not losing my lab notebook. Leighanne Gallington, for helping me figure out the nasty units of Einstein B coefficients and absorption cross sections. Peter Rigano, for help with proofreading. And to my four musketeers, Christine McEvilly, Anya Poukchanski, Amy Moore, and Jen Hogan, your M. de Tréville loves you all and you know why.

I must also acknowledge the wisdom imparted to me by the two teachers who taught me chemistry in high school: Corey Lowen and Jay Chandler. I decided to go into chemistry because of them, and I have used what they have taught me throughout my entire MIT career.

And finally my family. Thank you to my dad for understanding what I'm talking about during dinner, to my mother for changing the subject, and my brother for keeping me laughing.